Mon. Not. R. Astron. Soc. **375,** 673–684 (2007) doi:10.1111/j.1365-2966.2006.11328.x

A possible origin of the mass–metallicity relation of galaxies

J. Köppen,[1,2,3⋆] C. Weidner [4,5⋆] and P. Kroupa[5,6⋆]

[1]*UMR 7550, Observatoire Astronomique, 11 rue de l'Université, F-67000 Strasbourg, France*
[2]*Institut für Astronomie und Astrophysik der Universität Kiel, D-24098 Kiel, Germany*
[3]*International Space University, Parc d'Innovation, F-67400 Illkirch, France*
[4]*Departemento de Astronomía y Astrofísica, Pontificia Universidad Católica de Chile, Av. Vicuña MacKenna 4860, Macul, Santiago, Chile*
[5]*Argelander Institut für Astronomie der Universität Bonn, Auf dem Hügel 71, D-53121 Bonn, Germany*
[6]*The Rhine Stellar Dynamics Network (RSDN)*

Accepted 2006 November 21. Received 2006 November 20; in original form 2006 September 21

ABSTRACT

Observations show that galaxies follow a mass–metallicity relation over a wide range of masses. One currently favoured explanation is that less massive galaxies are less able to retain the gas and stellar ejecta and thus may lose the freshly produced metals in the form of galactic outflows. Galaxies with a low current star formation rate have been found to contain star clusters up to a lower mass limit. Since stars are predominately born in clusters, and less massive clusters have been found to be less likely to contain very massive stars, this implies that in environments or at times of low star formation, the stellar initial mass function does not extend to as high masses as during high star formation epochs. It is found that the oxygen yield is reduced by a factor of 30 when the star formation rate is decreased by 3 to 4 orders of magnitude. With this concept, chemical evolution models for galaxies of a range of masses are computed and shown to provide an excellent fit to the mass–metallicity relation derived recently by Tremonti et al. Furthermore, the models match the relation between galaxy mass and effective yield. Thus, the scenario of a variable integrated stellar initial mass function, which is based on the concept of formation of stars in clusters, may offer an attractive alternative or partial explanation of the mass–metallicity relation in galaxies.

Key words: stars: luminosity function, mass function – ISM: abundances – ISM: evolution – galaxies: abundances – galaxies: evolution – galaxies: ISM.

1 INTRODUCTION

It has been known for a long time that there exist fairly well-defined relations between the metallicity and mass (or luminosity) among gas-rich galaxies (Lequeux et al. 1979; Skillman, Kennicutt & Hodge 1989) as well as among gas-poor galaxies (Faber 1973; Brodie & Huchra 1991). Zaritsky, Kennicutt & Huchra (1994) point out the similarity of these relations, which is suggestive of a common physical origin of this phenomenon. Recently, the wealth of data from the Sloan Digital Sky Survey (SDSS) permitted Tremonti et al. (2004) to study the mass–metallicity relation over a wide range of masses and metallicities for about 53 000 star-forming galaxies.

Tremonti et al. (2004) interpret their data with a scenario of gas outflows which are stronger in dwarf galaxies. More massive galaxies are able to retain the gas longer and more effectively than low-mass objects, thus the metallicity can build up to higher values because following generations of stars will be formed in an enriched gas environment, while the low-mass objects lose their metals through galactic winds. Different amounts of dark matter can also assist in this process (Dekel & Silk 1986). De Lucia, Kauffmann & White (2004) show that the chemical evolution in hierarchical galaxy formation models is able to explain the observed mass–metallicity relation and other relations like the Tully–Fisher relation. This is achieved by including feedback processes like galactic winds into their cosmological simulations. The formulation of the feedback includes free parameters such as the feedback efficiency or the yield.

While galactic outflows are observed and this scenario provides a satisfactory match of the observed relation, one should not yet exclude other explanations or contributions from other processes. This is particularly important because the current galactic wind models still need to be individually fitted to the galaxies and are not easily explained by physical parameters of the galaxy. Furthermore, recent works by Lee et al. (2006) and Dalcanton (2006) show that simple outflows of interstellar medium (ISM) gas have difficulties reproducing the yields in dwarf galaxies. Lee et al. (2006) used observations with *Spitzer* to derive the mass–metallicity relation from a number of dwarf irregular galaxies. They conclude that the

⋆E-mail: koppen@astro.u-strasbg.fr (JK); cweidner@astro.puc.cl (CW); pavel@astro.uni-bonn.de (PK)

dispersion in the relation and the large variations in the effective yields 'are difficult to understand if galactic superwinds or outflows are responsible for low metallicities at low mass or luminosity'. In Dalcanton (2006), a series of closed-box chemical evolution models including infall and outflow is presented. There, it is shown that neither simple infall nor outflow can reproduce the observed low effective yields in low-mass galaxies, but metal-enriched outflows can do. That is, effectively the freshly synthesized elements need to be removed from the matter cycle, which is, in principle, equivalent to reducing the number of massive stars.

In this work, we like to further explore the implications of the fact that stars form predominantly in clusters (Lada & Lada 2003). Kroupa & Weidner (2003) showed that the integrated galactic initial mass function (IGIMF) of all stars in a galaxy depends on the embedded cluster mass function (ECMF), in the sense that more massive clusters are likely to have more massive stars, because of their greater amount of available gas to form stars. Based on the relation found by Weidner, Kroupa & Larsen (2004) between the maximum mass of clusters in a galaxy and the current star formation rate (SFR), Weidner & Kroupa (2005, 2006) show that the high-mass part of the resulting IGIMF is strongly dependent on the star formation history (SFH) in a galaxy, being in general steeper than the IMF. This gives an important influence on the production rate of metals (Weidner & Kroupa 2006). Goodwin & Pagel (2005) explored the effect of the IGIMF on the metal production in galaxies. They found a change in the general metal yield by a factor of $\sim$1.8 and by a factor of $\sim$1.5 for oxygen and magnesium when they use the ECMF slope of Lada & Lada (2003, i.e. $\beta = 2$).

One thus expects that the effective metal yields from the average stellar population may vary with time and galaxy type. It is not the aim of this contribution to exclude the scenario of galactic outflows, but to explore the possibilities and consequences arising purely from clustered star formation, and to probe to what extent it may provide an alternative or supporting explanation.

Section 2 briefly reviews the model of the SFR-dependent IGIMF (henceforth IGIMF for simplicity); Section 3 discusses the importance of the oxygen yields for this study, while in Section 4 the chemical evolution model is introduced and the effect of a variable IGIMF on the chemical evolution of galaxies is studied. In Section 5, the implications of these results are discussed, while Section 6 presents the conclusions from these results.

2 THE VARIABLE IMF

In Kroupa & Weidner (2003) and Weidner & Kroupa (2005, 2006), it has been shown that the formation of stars predominantly in clusters has a profound influence on the IGIMF of all stars in a galaxy. In contrast to the IGIMF, which is the 'IMF' integrated over a whole galaxy, the IMF of stars formed in a single cluster is well described by the well-known power-law function with the Salpeter/Massey slope $\alpha = 2.35$ (Salpeter 1955; Massey 2003) for stars more massive than $1\,\mathrm{M}_\odot$, as found in several observational studies (Massey & Hunter 1998; Sirianni et al. 2000, 2002; Parker et al. 2001; Massey 2002, 2003; Wyse et al. 2002; Bell et al. 2003; Piskunov et al. 2004), with

$$\xi(m) \propto m^{-\alpha_i}, \tag{1}$$

where $\xi(m)\,\mathrm{d}m$ is the number of stars in the mass interval $m, m + \mathrm{d}m$. Below $0.5\,\mathrm{M}_\odot$, the IMF is found to flatten (Miller & Scalo 1979; Scalo 1986; Kroupa, Tout & Gilmore 1993; Reid, Gizis & Hawley 2002), and the *standard* IMF becomes a segmented power law (Kroupa 2001, 2002):

$$\begin{aligned} \alpha_0 &= 0.30,\ 0.01 \leqslant m/\mathrm{M}_\odot < 0.08, \\ \alpha_1 &= 1.30,\ 0.08 \leqslant m/\mathrm{M}_\odot < 0.50, \\ \alpha_2 &= 2.35,\ 0.50 \leqslant m/\mathrm{M}_\odot \leqslant m_{\mathrm{max}*}. \end{aligned} \tag{2}$$

Note that this form constitutes a two-part power-law *stellar* IMF with the 'Salpeter/Massey' (or short 'Salpeter') slope above $0.5\,\mathrm{M}_\odot$. Note also that this form is similar to Kennicutt (1983) two-part power-law form, except that the slope at the high-mass end is less steep here (being the Salpeter/Massey value), and that the break in the power law occurs at a smaller mass here. These differences, while fairly subtle, are important as the form used here is based on a very thorough star-count analysis using post-1983 data (Kroupa et al. 1993; Kroupa 2001). The physical stellar upper mass limit is assumed to be $m_{\mathrm{max}*} = 150\,\mathrm{M}_\odot$, following the recent results by Weidner & Kroupa (2004), Figer (2005), Oey & Clarke (2005) and Koen (2006).

The masses of young, embedded star clusters also follow a power-law distribution, the ECMF

$$\xi_{\mathrm{ecl}}(M_{\mathrm{ecl}}) \propto M_{\mathrm{ecl}}^{-\beta}, \tag{3}$$

where $\xi_{\mathrm{ecl}}(M_{\mathrm{ecl}})\,\mathrm{d}M_{\mathrm{ecl}}$ is the number of embedded clusters in the mass interval $(M_{\mathrm{ecl}}, M_{\mathrm{ecl}} + \mathrm{d}\,M_{\mathrm{ecl}})$, and M_{ecl} is the mass in stars. Lada & Lada (2003) find a slope $\beta \approx 2$ in the solar neighbourhood for clusters with masses between 50 and $1000\,\mathrm{M}_\odot$, while Hunter et al. (2003) find $2 \lesssim \beta \lesssim 2.4$ for $10^3 \lesssim M_{\mathrm{ecl}}/\mathrm{M}_\odot \lesssim 10^4$ in the Small Magellanic Cloud (SMC) and Large Magellanic Cloud (LMC), Zhang & Fall (1999) find 1.95 ± 0.03 for $10^4 \lesssim M_{\mathrm{ecl}}/\mathrm{M}_\odot \lesssim 10^6$ in the Antennae galaxies. Weidner et al. (2004) find that $\beta = 2.35$ best reproduces the observed correlation between the brightest young cluster and the global SFR for a sample of late-type galaxies.

The IMF of all stars ever formed in a galaxy (the IGIMF) is obtained by summing up all standard IMFs of all clusters from which a galaxy is formed,

$$\xi_{\mathrm{IGIMF}}(m) = \int_{M_{\mathrm{ecl,min}}}^{M_{\mathrm{ecl,max}}} \xi[m \leqslant m_{\mathrm{max}}(M_{\mathrm{ecl}})]\,\xi_{\mathrm{ecl}}(M_{\mathrm{ecl}})\,\mathrm{d}M_{\mathrm{ecl}}, \tag{4}$$

where $\xi_{\mathrm{ecl}}(M_{\mathrm{ecl}})$ is the ECMF and $\xi[m \leqslant m_{\mathrm{max}}(M_{\mathrm{ecl}})]$ is the stellar IMF in a particular cluster within which the maximal mass of a star is m_{max}. A critical ingredient of this concept is the existence of the correlation between the maximum stellar mass m_{max} and the cluster mass M_{ecl}, which depends on the sequence with which stars of different masses are formed. Weidner & Kroupa (2006) find that several young clusters are best described if one assumes that, starting at the lowest mass, stars of progressively higher mass are formed.

In Fig. 1, we show an example of the resulting IGIMF from equation (4), using an ECMF power-law slope $\beta = 2.2$. Note that the IGIMF (*dashed line*), which has a slope above $1.5\,\mathrm{M}_\odot$ of about 2.77, is steeper than the standard IMF (*dotted line*); furthermore it turns down rather sharply near $m_{\mathrm{max}*} = 150\ \mathrm{M}_\odot$, the fundamental upper mass limit for stars (Weidner & Kroupa 2004, 2005; Figer 2005; Oey & Clarke 2005; Koen 2006).

Elmegreen (2006) puts forward the view that the IGIMF equals the IMF, but we note that his discussion points to a few examples which actually do impose a variable IGIMF. Our formulation tests, like that of Elmegreen, the case of $\beta = 2$, but ours allows a variation of the maximum mass of the stars with the SFR, in contrast to Elmegreen's where this mass comes out to be constant.

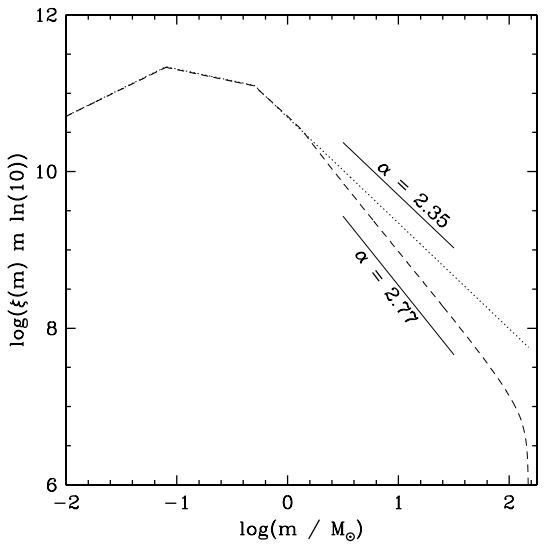

Figure 1. The dotted line is the standard IMF $\xi(m)$, given by equation (2) which has $\alpha = 2.35$ for $m > 0.5\,\mathrm{M}_\odot$. The dashed line is the overall IGIMF, $\xi_{\mathrm{IGIMF}}(m)$, for $\beta = 2.2$. All functions are scaled to have the same number of objects in the mass interval 0.01–1.0 $\mathrm{M}_\odot$. Slopes $\alpha = 2.35$ and 2.77 are indicated by lines. Note that we use the notation $\log = \log_{10}$ throughout the paper.

2.1 The connection to the SFR

The IGIMF depends not only on the ECMF but also on the SFH of a galaxy. Weidner et al. (2004) derive a relation between the current SFR and the maximum mass of a cluster in a galaxy. With this relation

$$\log M_{\mathrm{ecl,max}}(t) = \log k_{\mathrm{ML}} + 0.75 \log \mathrm{SFR}(t) + 6.77, \qquad (5)$$

and a mass-to-light ratio of $k_{\mathrm{ML}} = 0.0144$, typically for young (<6 Myr) clusters, the IGIMF evaluated during the time interval $t, t + \delta t$ – with the (constant) 'star formation epoch' $\delta t = 10$ Myr (Weidner & Kroupa 2005) – becomes

$$\xi_{\mathrm{IGIMF}}[m, \mathrm{SFR}(t)] = \int_{M_{\mathrm{ecl,min}}}^{M_{\mathrm{ecl,max}}[\mathrm{SFR}(t)]} \xi[m \leqslant m_{\mathrm{max}}(M_{\mathrm{ecl}})]\, \xi_{\mathrm{ecl}}(M_{\mathrm{ecl}})\, \mathrm{d}M_{\mathrm{ecl}}. \qquad (6)$$

A similar time-scale δt is found by Egusa, Sofue & Nakanishi (2004) from measuring the offset of H II regions from the dark spiral arms in a number of galaxies. In our interpretation, δt is the time-scale within which an ECMF is completely populated. This result is at least qualitatively supported by Elmegreen (2000). By comparing the observational properties of embedded clusters and molecular clouds, he derives 'that star formation occurs in only one or two crossing times'. Hartmann, Ballesteros-Paredes & Bergin (2001) also argue for short, less than a few Myr, molecular-cloud lifetimes; and the Antennae (Zhang & Fall 1999) have a fully developed cluster MF at an age of ∼10 Myr. Thus, a lower SFR results in a lower maximum cluster mass which essentially reduces the upper mass limit for the stars.

Note that equation (6) is the correct 'IMF' to be used when studying the global SFR properties of galaxies. Kennicutt (1983), for example, finds $\alpha = 2.5$ (for $m > 1\,\mathrm{M}_\odot$) reproduces integrated luminosities of star-forming galaxies. Although he refers to this 'IMF' as a 'Salpeter IMF', it is actually a steeper function (with a larger α).

2.2 Model parameters

Because the IGIMF is steeper than Salpeter's IMF, which is often used in chemical evolution studies, its dependence on the SFR can be expected to have observable consequences for the chemical enrichment of galaxies. For our evolution models, we will use the following parameters:

(i) minimum mass of the clusters: $M_{\mathrm{ecl,min}} = 5\,\mathrm{M}_\odot$. This corresponds to a Taurus–Auriga star-forming 'cluster' containing a dozen stars,
(ii) range of 'stellar' masses: 0.01 to 150 $\mathrm{M}_\odot$,
(iii) ECMF power-law exponent $\beta = 2$ and also 2.35 and
(iv) the standard IMF (equation 2).

The IGIMFs obtained for various SFRs are displayed in Fig. 2 in the form of number of stars per unit stellar mass interval (Salpeter's IMF has the exponent 2.35). A lower SFR reduces the maximum cluster mass and hence the upper mass limit for the stars; this is quite a strong effect. One also notes the steepening of the slope, especially at high stellar masses.

In Fig 3, we show that the slope β of the cluster mass function also affects the slope of the IGIMF above stellar masses of 1 $\mathrm{M}_\odot$. For the same SFR, the upper mass limit does not change, however increasing β further steepens the IGIMF slope. To display this dependence, we took a larger range of values for β than indicated from observations.

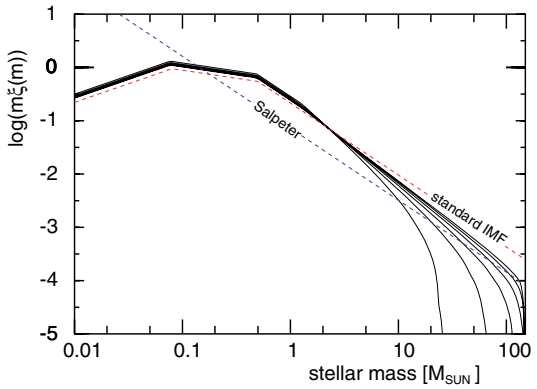

Figure 2. The IGIMFs computed for SFR = 0.01, 0.1, 1, 10 and 100 $\mathrm{M}_\odot\,\mathrm{yr}^{-1}$ (solid lines, from bottom to top) *and* $\beta = 2$, compared to the Salpeter IMF for the entire stellar mass range 0.01 to 150 $\mathrm{M}_\odot$. All IMFs are normalized to have the same number of stars in the interval 0.01 to 150 $\mathrm{M}_\odot$. The standard IMF is equation (2).

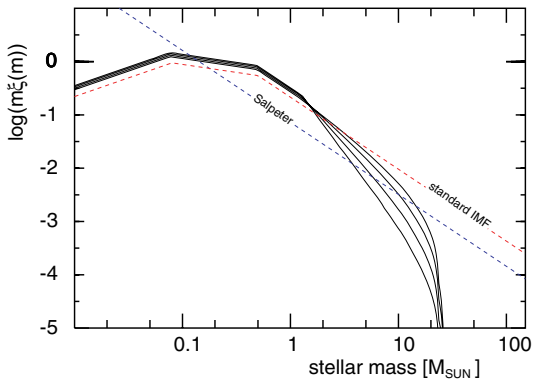

Figure 3. Like Fig. 2, but for the same SFR = 0.01 $\mathrm{M}_\odot\,\mathrm{yr}^{-1}$ and $\beta = 1.65, 2.0, 2.35$ and 2.7 (solid lines, from right- to left-hand side).

3 OXYGEN YIELDS

From the IGIMFs, we compute the yields of oxygen by integrating over the entire stellar mass spectrum the stellar yields weighted with the IGIMFs (cf. e.g. Köppen & Arimoto 1991). The prescriptions for the stellar nucleosynthesis are: for massive stars we use Thielemann, Nomoto & Hashimoto (1996), including the yields for the $40\,M_\odot$ star quoted by Thomas, Greggio & Bender (1998); beyond $40\,M_\odot$ we assume that the mass fractions of freshly produced elements are constant. For low- and intermediate-mass stars, we take van den Hoek & Groenewegen (1997). This choice is known to give a good match to the chemical evolution of the solar neighbourhood, if one uses a Salpeter IMF (cf. e.g. Thomas et al. 1998), because the yield is close to the solar oxygen abundance. As will be shown by the results below (Fig. 11), this choice also gives a good match with the observational data for galaxy masses of $10^{11}\,M_\odot$. Uncertainties in the stellar yields would amount to at least a factor of 2 (e.g. Henry, Edmunds & Köppen 2000) to be applied in either direction.

The oxygen yield (Fig. 4) decreases strongly when the SFR is below about $1\,M_\odot\,yr^{-1}$. This mirrors the strong dependence of the upper mass limit on the SFR. Test calculations show that the influence of the variation of the IGIMF slope with SFR is of less importance. Since for high values of the SFR the IGIMF approaches the standard IMF (cf. Fig. 2), the yield converges towards the value obtained with the full standard IMF sampled to the maximum cluster mass. The yields also depend on the assumed value for β; larger values result in IGIMFs more strongly cut-off at the high-mass end. In the figure, we show – to illustrate this dependence – a greater range of values for β than suggested by observations (2.0, ... , 2.35; cf. Section 2). A Salpeter IMF for the entire stellar mass range gives an oxygen yield very close to the solar oxygen abundance. As the oxygen yields from massive stars depend on the stellar metallicity only very weakly (see Woosley & Weaver 1995), our results computed for solar composition stars also apply to non-solar metallicities.

Stellar oxygen yields of stars as massive as $40\,M_\odot$ are less certain due to the poor knowledge about the explosion characteristics (Woosley & Weaver 1995). Furthermore, our adopted nucleosynthesis recipe extrapolates the stellar yields beyond $70\,M_\odot$. We investigated the influence of these uncertainties by computing the yields under the assumption that oxygen is ejected only by stars below a certain upper mass limit. As depicted in Fig. 5, the resulting yields are reduced by about a factor of 2, if oxygen is produced only by stars less than $40\,M_\odot$. The dependence on the SFR becomes somewhat less steep for low values of the SFR.

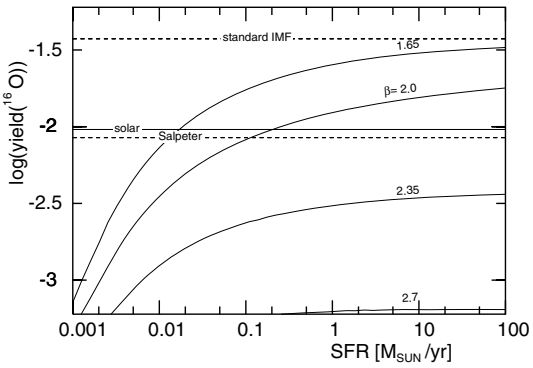

Figure 4. Oxygen yields as a function of the SFR for several values of β. The yields for a Salpeter IMF over all stellar masses and the standard IMF (equation 2) are shown by horizontal dashed lines.

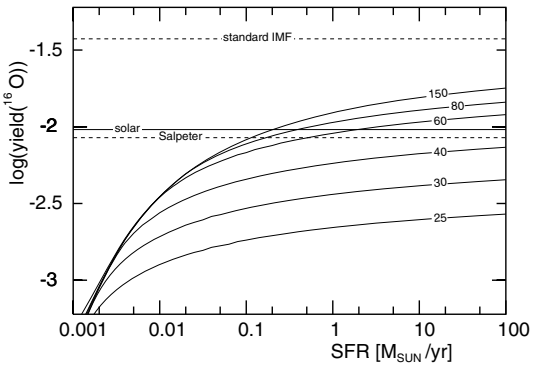

Figure 5. Same as Fig. 4, but for $\beta = 2$ and several values for the upper mass limit for oxygen production in massive stars (from 150 to $25\,M_\odot$).

If all galaxies had the same age of about 10 Gyr, galaxies with masses between 10^7 and $10^{11}\,M_\odot$ have time-averaged SFRs ranging from 0.001 to $10\,M_\odot\,yr^{-1}$ (cf. Fig. 4). Since over this interval, the oxygen yield increases by about a factor of 30, we may thus expect that the SFR-dependent IGIMF causes observable effects in the chemical evolution of these systems.

4 CHEMICAL EVOLUTION MODELS FOR GALAXIES OF DIFFERENT MASSES

In order to study the effects of the SFR-dependent IGIMF on the present-day gas abundances of galaxies of different masses, we compute a series of illustrative chemical evolution models to display the principal effects and show their magnitude. These models use simple parametrizations, and thus are not designed to match the exact time histories of the galaxies; however we concentrate on those properties – metallicity and gas fraction – in which chemical evolution models are known to be less sensitive to modelling details. Thus, the results retain a certain degree of general validity.

4.1 Physical assumptions

Each galaxy is treated as a one-zone model, dealing with the gas return and metal production of stars of different masses in detail and taking into account the finite lifetimes of the stars. The ejected gas and metals are assumed to be mixed perfectly and instantaneously with the gas in the model, as is done in the usual chemical evolution studies (cf. e.g. Talbot & Arnett 1971; Matteucci 1986). As described before, the stellar nucleosynthesis prescriptions are from Thielemann et al. (1996) for massive stars (type II supernovae) and van den Hoek & Groenewegen (1997) for low- and intermediate-mass stars.

At each time-step, the IGIMF is selected in accordance with the current value of the SFR, using a pre-computed lookup table. The SFR has the same form as used by, e.g., Matteucci & Francois (1992),

$$\mathrm{SFR}(t) = \frac{M_{\mathrm{gas}}(t) + M_{\mathrm{stars}}(t)}{\tau_{\mathrm{SFR}}} \left[\frac{M_{\mathrm{gas}}(t)}{M_{\mathrm{gas}}(t) + M_{\mathrm{stars}}(t)} \right]^x , \qquad (7)$$

which depends on the current masses of gas, $M_{\mathrm{gas}}(t)$, and stars, $M_{\mathrm{stars}}(t)$, and thus on the current values of total mass and gas fraction. The parameter x is taken as unity, although test calculations are done with other values, giving very similar results, provided the present-day gas fraction remains the same, as one should expect for closed-box and infall models. The star formation time-scale τ_{SFR} is

assumed to be the same for all galaxy masses; several values will be taken, which will thus determine the present gas fraction. In later models, we will allow $\tau_{\rm SFR}$ to vary with galaxy mass.

The galaxy is treated either as a closed box with all its initial mass in the form of metal-free gas or as an infall model where the primordial gas is accreted with a rate that decreases exponentially in time:

$$\dot{M}(t) = M_{\rm gal}\frac{\exp(-t/\tau_f)}{1-\exp(-T/\tau_f)}, \tag{8}$$

with the time-scale $\tau_f = 5$ Gyr, similar to that of Matteucci & Francois (1992) and Thomas et al. (1998) for models of the solar neighbourhood. We assume all the mass of the gas to be accreted within the age $T = 13$ Gyr of the galaxy. It is worth pointing out that with this kind of monotonic gas infall, the oxygen abundance remains close to the values from a closed-box model of the same gas fractions (Köppen & Edmunds 1999). Thus, the choice of the infall time-scale is of minor importance in the context of the primary element oxygen ejected with very little time delay.

For the numerical calculations, we use a grid of 190 logarithmically spaced stellar masses and 500 time-steps to cover 13 Gyr.

4.2 Closed-box models

We first compute a series of closed-box models. The star formation time-scale is taken to be a fraction or multiple of the age of the galaxy: $\tau_{\rm SFR} = T/a$. The factor a is assumed to take values of 0.5, 1, 2, 3 and 4, i.e. time-scales of 26, 13, 7, 3.5 and 1.75 Gyr. These five series of models with different galactic masses span a rather wide range of present-day gas fractions,

$$f_{\rm gas}(T) = \frac{M_{\rm gas}(T)}{M_{\rm gas}(T)+M_{\rm stars}(T)}. \tag{9}$$

In Fig. 6, we compare these models with the data of Tremonti et al. (2004) for the relation between stellar mass of the galaxies and gas-phase oxygen abundance. The computed relations are somewhat flatter than the observed relation, but models with present-day gas fractions between 25 and 50 per cent are indeed well suited

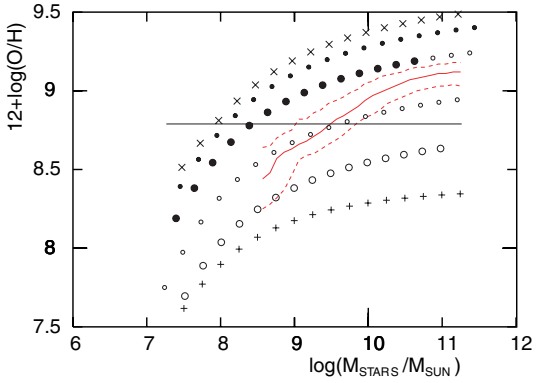

Figure 6. The relation between oxygen abundance and stellar mass of galaxies. Dashed lines indicate the 16, 50 and 84 percentiles of the observed metallicity distribution by Tremonti et al. (2004). The symbols are results from closed-box models: from top to bottom, the model series (with $\beta = 2$) correspond to the factor a in the SFR to 4, 3, 2, 1 and 0.5. The symbols indicate the present-day gas fraction: large circles >0.5, small circles 0.5, . . . , 0.25, large filled circles 0.25, . . . , 0.15, small filled circles 0.15, . . . , 0.1 and crosses <0.1. The plus signs show the model series with $a = 1$ but $\beta = 2.35$. The full horizontal line refers to a model grid obtained with a constant Salpeter IMF between 0.01 and 150 $M_\odot$.

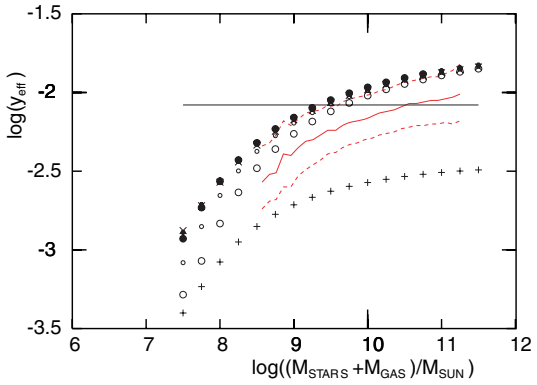

Figure 7. The relation between the effective Oxygen yields and the total galactic mass: dashed lines indicate the 16, 50 and 84 percentiles of the observed distribution by Tremonti et al. (2004). The symbols denote the same sequences of closed-box models of Fig. 6. The horizontal line refers to models with a constant Salpeter IMF. The plus signs show the model series with $a = 1$ but $\beta = 2.35$.

to explain the observed metallicities, which correspond to $a \approx 1$. For comparison, we show one model series done with a constant Salpeter IMF. Since in these models the oxygen abundance is a function of only the gas fraction which is determined by the star formation time-scale, each of the five model series gives an oxygen abundance independent of the galactic mass. The model shown is done with $a = 1$, the other models result in horizontal lines at different oxygen abundances, ranging from 8.5 for $a = 0.25$ to 9.4 for $a = 4$.

Tremonti et al. (2004) also determine the relation between total galaxy mass $M_{\rm gal} = M_{\rm gas}(T) + M_{\rm stars}(T)$ and the effective oxygen yield, which they compute from current oxygen abundances and gas fractions by assuming a closed-box model,

$$y_{\rm eff} = -\frac{Z(^{16}{\rm O})}{\ln f_{\rm gas}(T)}. \tag{10}$$

Our closed-box model sequences (Fig. 7) reproduce the slope of the relation remarkably well, although being higher than the median observed relation by 0.1 dex. This is in strong contrast to models with a constant IMF which all have the same effective yield for all galactic masses and all star formation time-scales.

4.3 Infall models

Motivated from chemical evolution models for the solar neighbourhood, we consider continuous infall of primordial gas (e.g. Matteucci & Francois 1992; Thomas et al. 1998; Naab & Ostriker 2006). The infall rate is assumed to decrease exponentially in time with a time constant of 5 Gyr. As can be seen from Fig. 8, one obtains larger gas fractions and lower metallicities. Thus, models with $a \approx 2$ are quite suitable. We note that infall does not change the slope of the relation which remains slightly too flat.

As expected for models with monotonically decreasing infall, the effective yields are only slightly (less than 0.1 dex) lower than found from the closed-box models. Hence, they also match the shape of the observed median relation remarkably well.

Since a general trend is observed that massive galaxies have smaller gas fractions than dwarfs (e.g. Köppen & Hensler 2005), we construct another set of models in which the star formation time-scale is assumed to decrease with increasing galactic mass $M_{\rm gal}$ in

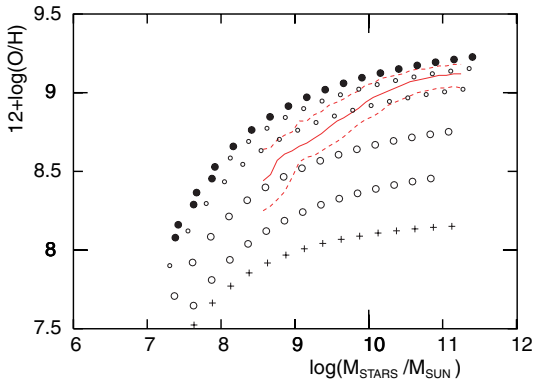

Figure 8. Same as Fig. 6 but for models with an exponentially decreasing infall of primordial gas.

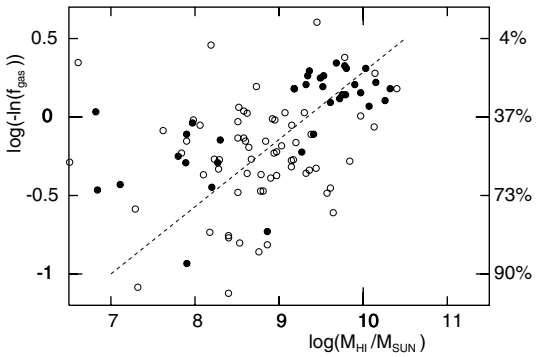

Figure 9. The observed relation of hydrogen mass and gas fraction [adapted from Köppen & Hensler (2005) where details may be found]. The filled dots mark objects with gas fractions determined by Garnett (2002) that account for both atomic and molecular content. The dotted line is an assumed relation, used for Fig. 19.

such a way,

$$\tau_{\rm SFR} = 20\ {\rm Gyr}\ \left(\frac{M_{\rm gal}}{10^8\ {\rm M}_\odot}\right)^{-0.3}, \qquad (11)$$

that the observed data (Fig. 9) are reasonably well matched. In Fig. 10, we show three model sequences, done with the above time-scale, as well as with half and twice its value. For comparison, we also compute three model sequences with a constant Salpeter IMF. A similar dependence of the SFR time-scale on galactic mass [$\tau_{\rm SFR} = 50\,{\rm Gyr}\ (M_{\rm gal}/10^8\ {\rm M}_\odot)^{-0.25}$] gives a satisfactory match to the observations.

The resulting model sequences match very well the distribution observed by Tremonti et al. (2004), as is seen in Fig. 11. It is worth noting that the agreement is excellent in terms of both slope and metallicity.

The effective yields (Fig. 12) also match the observed relation very reasonably, although the slope among the massive galaxies is flatter and even turns down, and near $10^{9.5}\ {\rm M}_\odot$ the yields are about 0.1 dex too large.

The adopted infall time-scale is not a critical parameter for this match with observations: monotonically decreasing infall leads to but minor deviations from the closed-box model properties, in particular the relation between gas fraction and metallicity. As is evident from Figs 6 and 8, the metallicity in more massive galaxies is decreased by about 0.2 dex; but it is worth emphasizing that the locus of the galaxies with the *same gas fraction* has hardly changed at

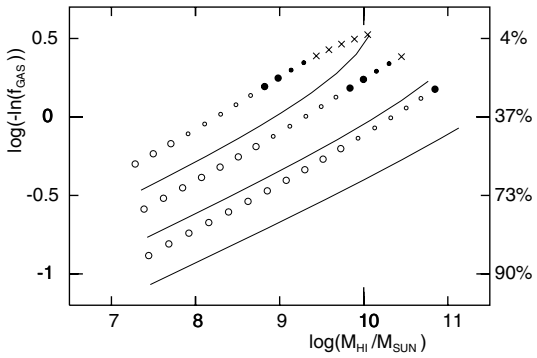

Figure 10. The relation between present gas mass and gas fraction from models with gas infall of 5 Gyr time-scale. The central series of symbols refers to star formation time-scales which depend on the galaxy's mass following equation (11). The SFR time-scales are halved in the upper series and doubled for the lower sequence. The meaning of the symbols is as in Fig. 6. The three full lines are for similar models, but computed with a constant Salpeter IMF.

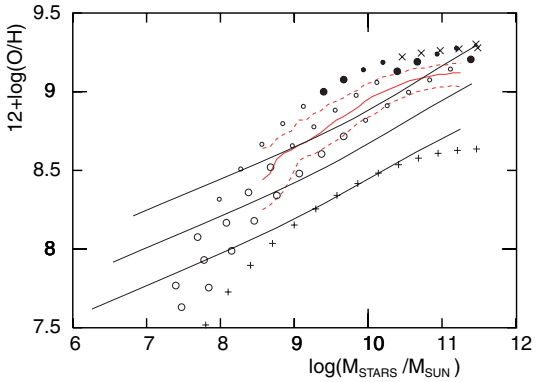

Figure 11. Similar to Fig. 6 but for models with exponentially decreasing infall of primordial gas and with a SFR depending on the galactic mass (equations 7 and 11). The three series of models are as in Fig. 10. The full curves refer to a model computed with a constant Salpeter IMF, while the plus signs show the model series with $a = 1$ but $\beta = 2.35$.

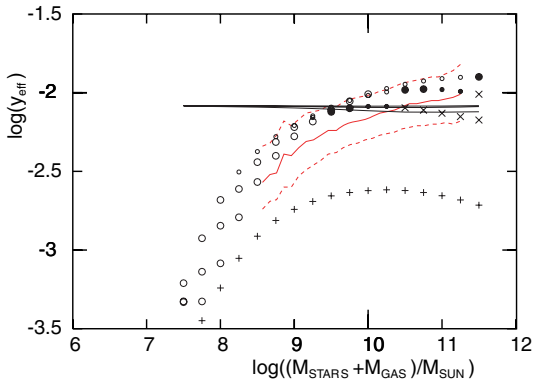

Figure 12. Similar to Fig. 7, but for the infall models of Fig. 10. The symbols are the same as in Fig. 6. The nearly horizontal curves are from the models computed with a constant Salpeter IMF.

all. The same holds true if one chooses the infall time-scale to be anywhere between about 1 and 10 Gyr.

The models with a constant IMF do not provide such a good match: while the assumed relation between SFR time-scale and

galactic mass could account for an increase of metallicity with galactic mass, our simple recipe cannot reproduce the shape of the observed relation (Fig. 11). Furthermore, these models completely fail to match the mass–effective-yield relation, as their yields are nearly independent of galactic mass (Fig. 12). Thus, the dependence of effective yield on galaxy mass might be more crucial in tracing the origins of the mass–metallicity relation.

4.4 Models with starbursts

Among dwarf irregular galaxies, the SFH is known to show strong temporal variations (e.g. Grebel 2001). How does the presence of star bursts influence the results? Let us consider the extreme case that all star formation occurs in short periods with long intervals of no star formation. We will assume that in galaxies with less than $10^{10}\,M_{\odot}$ stars are formed in a burst lasting 100 Myr every 1 Gyr. In order to obtain the same present gas fraction as in a model with continuous star formation, the SFR during the short bursts must be 30 times higher than the average rate. The resulting IGIMF contains a larger fraction of massive stars, and thus the average metal yield will be higher than under continuous star formation. Thus, strong starbursts lead to both higher oxygen abundances (Fig. 13) and higher effective yields (Fig. 14), as shown in this somewhat extreme model. One notes that since for these models the SFR is higher, the variations of the upper stellar mass limit and the IGIMF slope should be milder. As shown in Fig. 14, the variation of the effective oxygen yield is less than in the models with continuous star formation (cf. Fig. 12). In the oxygen abundances, this change is much less apparent, because the assumed dependence of the SFR time-scale on galactic mass (equation 11) contributes fairly strongly to the mass–metallicity relation (cf. Fig. 11).

We emphasize that this schematic modelling of star formation bursts serves to show the influence on the results of a rather extreme burst-type history of star formation, irrespective of the physical processes which could form the base for such a behaviour. The parameters were chosen to provide a clear demonstration of the effects. None the less, the results predict that with a SFR-dependent IGIMF one would expect that galaxies which had a strongly fluctuating SFH would tend to have higher metallicities and higher oxygen yields.

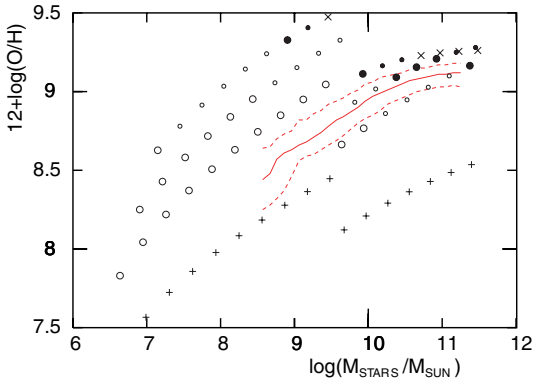

Figure 13. Like Fig. 11 but assuming that for galaxies with a *total* mass below $10^{10}\,M_{\odot}$ star formation occurs in bursts of 100 Myr duration every 1 Gyr. During a burst, the SFR is 30 times higher than the average rate.

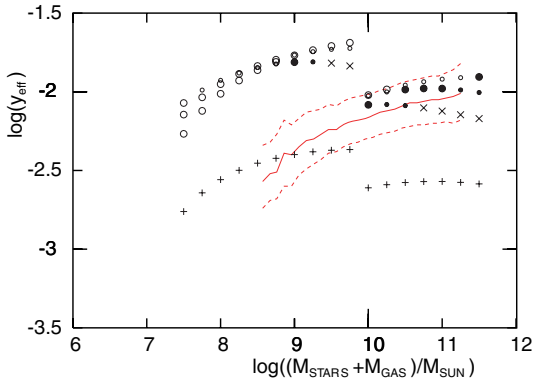

Figure 14. Like Fig. 12 but assuming that for galaxies with a *total* mass below $10^{10}\,M_{\odot}$ star formation occurs in bursts of 100 Myr duration every 1 Gyr. During a burst, the SFR is 30 times higher than the average rate.

5 DISCUSSION

5.1 Chemical evolution models

The consequences of the IGIMF depending on the SFR is primarily that the oxygen yield is higher in environments – or times – where the SFR is high. Thus, more massive galaxies are expected to have higher yields and thus have a tendency to have higher metallicities. This basic implication is quantified in the chemical evolution models presented in Section 4.

(i) The closed-box models exhibit mass–metallicity and mass–yield relations which are very similar to what is observed, without the need to invoke additional physics.

(ii) Adding infall of primordial gas modifies both relations only slightly. The presence of gas infall or the true history of the infall – as long as it decreases monotonically in time – is not crucial for this comparison.

(iii) If the observed trend between galaxy mass and present gas fraction is matched by adopting a dependence of the star formation time-scale on galaxy mass, both observed relations of Tremonti et al. (2004) can be reproduced very well. This supplementary assumption leads to a further improvement of the fit of the mass–metallicity relation, but it is not an essential ingredient, because it alone cannot account for the mass-effective-yield relation.

Thus, the main contribution to the agreement with the Tremonti et al. (2004) data is the variable IGIMF, and not the details of the model.

5.2 Star formation history

We have chosen a rather simple recipe for the SFR and adopted a dependence of its time-scale on galaxy mass on the basis of matching the observed trend in the current gas fractions on galaxy mass. Chemical evolution models with constant yield but gas infall remain rather close to the relation of the closed-box model, unless subjected to massive and rapid inflow of gas (Köppen & Edmunds 1999; Köppen & Hensler 2005). Because oxygen is an element whose enrichment occurs with negligible time delays, its present abundance is predominantly determined by the gas fraction, but irrespective of the time dependence of the SFR.

This also applies to our models with a variable IMF and *continuous* star formation: in massive galaxies with their high SFR the yield is rather insensitive to changes in the SFR (Fig. 4). The instantaneous yield changes very little in the course of time, as evident, for example, in Fig. 7: only for low galaxy masses do the models with different a give different effective yields, because during its time

evolution the low SFR results in a strong change of the yield. Although in the models the IGIMF depends both on time and on galaxy mass, it is the dependence on the latter parameter which clearly dominates. Therefore one has a direct mapping of the SFR–yield relation into the mass–effective-yield relation, as the close similarity of the curves in Figs 4 and 7 shows. Furthermore, models with a constant star formation time-scale have the same gas fraction for all galaxy masses, hence the closed-box relation $Z = -y\ \ln(f_{\rm gas})$ provides a common scaling factor between yield and abundance (Fig. 6).

Therefore, as far as a continuous star formation is concerned, a comparison of its history predicted by our models with observations does not constitute a critical test of their validity or of the variable IMF concept. The presence of burst-like forms of star formation and the consequences in conjunction with a variable IMF is addressed later in this section. But it is worth noting that the time-scale for star formation in the Universe is found to be about 7 Gyr (Glazebrook et al. 2003; Brinchmann et al. 2004) and that models with such a value (i.e. $a = 2$) match quite well the observed mass–metallicity relation (Figs 6 and 8). The reason is the already mentioned simple mapping of the SFR–yield relation into the mass–metallicity relation: with a value of 7 Gyr, a closed-box model with linear SFR ($x = 1$) gives a present gas fraction of $f^{\,0}_{\rm gas} = 0.13$. Since the gas fraction and thus the SFR decrease exponentially, a galaxy of $M_{\rm gal} = 10^{10}\,{\rm M}_\odot$ has an average SFR of $M_{\rm gal}(1 - f^0_{\rm gas})/13\,{\rm Gyr} = 0.67\,{\rm M}_\odot\ {\rm yr}^{-1}$. From Fig. 4, one obtains a yield slightly above solar value. The closed-box relation then gives the oxygen abundance $Z = -y\ \ln(f_{\rm gas})$ as about twice the yield, as is seen in Fig. 6.

Observational data are available to compare with our adopted relation between star formation time-scale and galaxy mass: Heavens et al. (2004) determine the stellar populations in nearly 100 000 galaxies from the continua observed in the SDSS and deduce the time dependence of the SFR in galaxies as a function of their mass. While galaxies with masses of less than $10^{10}\,{\rm M}_\odot$ have star formation increasing slightly with time, which might indicate a very slow infall of gas, the SFR for, e.g., $10^{11}\,{\rm M}_\odot$ is initially about 100 times higher and declines rapidly, with a time-scale of about 1, . . . , 2 Gyr. This behaviour also implies that today's low-mass galaxies remain richer in gas than the massive systems. Our recipe gives a similar value of 2.5 Gyr for $10^{11}\,{\rm M}_\odot$, but with 5 Gyr for $10^{10}\,{\rm M}_\odot$ the gas consumption is too rapid. For lower masses, our time-scale increases and thus the SFH is dominated by the infall which results in a nearly constant or increasing rate. This can be considered consistent with the data of Heavens et al. (2004) which lump all masses below $10^{10}\,{\rm M}_\odot$ in a single bin.

In a sample of the same size, Brinchmann et al. (2004) find that for masses below about $10^{10}\,{\rm M}_\odot$ the SFR has a tight relation with the stellar mass in a galaxy (their fig. 17). However, the high ratios of present and average past SFR confirm that star formation is dominated by bursts, and therefore its current value is not necessarily representative for the average rate of gas consumption. Therefore, for more detailed modelling of these galaxies the SFR recipe would need to include a proper description of the burst-type nature of star formation.

We have refrained from doing this in the present work, but in Section 4.4 we illustrate the effects of starbursts on the results. In this extreme model with ${\rm SFR}/\langle{\rm SFR}\rangle = 30$, which is about 10 times larger than the largest value shown in fig. 24 of Brinchmann et al. (2004), the effective yield and the oxygen abundance for galaxies with $<10^{10}\,{\rm M}_\odot$ are enhanced by about 0.4 dex. Since these galaxies have ${\rm SFR} < 0.7\,{\rm M}_\odot\ {\rm yr}^{-1}$, we see from Fig. 4 that the yield increases by 0.3, . . . , 0.4 dex for an increase of a factor of 30 in the SFR, and 0.1, . . . , 0.2 dex for a factor of 3. Thus the enhancements would be less than half of those shown in Figs 13 and 14. The results of Brinchmann et al. (2004) would imply that while at masses near $10^{10}\,{\rm M}_\odot$ there would a negligible change from our results but that due to the effects of starbursts the effective yields and the oxygen abundances would progressively be enhanced for lower masses, amounting to about 0.2 dex at $10^8\,{\rm M}_\odot$. The low-mass branch in both relations would be somewhat flatter than predicted from our continuous star formation models. However, this difference remains comparable with the uncertainties of the stellar nucleosynthesis prescriptions and of the observational data, to be discussed in the subsequent sections.

5.3 Oxygen abundances

The absolute values of abundances and yields from the models depend on the adopted recipes for the stellar nucleosynthesis, which may differ in the underlying stellar physics, such as the treatment of convection, the nuclear cross-sections and the explosion characteristics. For example, the stellar oxygen yields from Thielemann et al. (1996) and Woosley & Weaver (1995) can differ for the same stellar mass by as much as a factor of 2, as shown by Thomas et al. (1998). Other effects, such as stellar mass loss (Maeder 1992) and rotation (e.g. Meynet & Maeder 2002), also have a strong influence on the stellar yields. In view of these uncertainties as well as of those in the observational data, which are addressed below, the agreement of the absolute abundance values between our models and the data of Tremonti et al. (2004) should be regarded but as a welcome aspect. The essential feature of the variable IMF models is the agreement in the overall shape of both relations, already apparent in the closed-box models.

5.4 Galaxy formation

One basic assumption in the models is that the SFH of a galaxy is governed by an overall time-scale. If galaxies form as isolated entities, one could expect such a behaviour. If – to take the hierarchical galaxy formation to a limiting case – all stars were formed in smaller substructures and in the same way, from which galaxies are built by mere additions, one should expect that all galaxies should have the same present gas fraction. The variation of gas fractions and present star formation among spiral and irregular galaxies gives evidence that a substantial star formation must have taken place during or after the assembly of a galaxy. In the first place, a more massive galaxy would have undergone a larger number of star formation episodes which could well result in an overall relation between star formation and present galactic mass. What fractions of stars are formed in either of these two modes is not yet clear. Conselice (2006) finds that most of today's massive galaxies probably have accreted the majority of their mass in only four or five major mergers in the early universe. As the merging objects must already have been quite massive ($\sim 2 \times 10^{10}\,{\rm M}_\odot$ in baryons) and young, the resulting IGIMF would be quite similar to the final IGIMF as the change in the IGIMF is most prominent for galaxies below $10^{10}\,{\rm M}_\odot$ (Weidner & Kroupa 2005). Unavane, Wyse & Gilmore (1996) and Venn et al. (2004) have shown that the Milky Way stellar population has abundance patterns that cannot be derived from accreted satellites, unless they had significantly different stellar populations than today's dwarf spheroidal galaxies. This, however, would be unphysical, because $\leqslant 10^7\,{\rm M}_\odot$ satellites would not be able to chemically enrich the Milky Way values.

If a major portion of the present stellar population was formed in smaller substructures, probably with a high SFR, or if each merging

of a substructure results in an episode of enhanced star formation, one should expect higher values for the average effective yield and the metallicity – as demonstrated in the models with bursty star formation histories. Thus, the variation of the metallicities could be less than computed from our models.

Our models – closed box and infall – thus constitute an upper limit of the effects due to a variation of the IGIMF on the SFR.

5.5 Galactic outflows

The effective yields can further be reduced by the loss of metals due to galactic winds. While the details of the effects of supernova explosions on the chemical evolution are quite complex (e.g. Mac Low & Ferrara 1999; Recchi et al. 2006), one may distinguish two simplified cases:

Some part of the metal-rich ejecta freshly produced by the massive stars are directly expelled from the galaxy. How large this fraction is depends on the details of the explosion, the multiphase structure of the ISM and the location in the galaxy (see e.g. Freyer, Hensler & Yorke 2003), which makes it difficult to give reliable estimates. It is obvious, however, that the effective yield could be reduced to arbitrarily small values, as it might be possible that *all* stellar ejecta leave the galaxy. Indeed, this issue is unclear, as Silich & Tenorio-Tagle (1998, 2001) show that even massive galaxies would lose all their metals through outflows if the Mac Low & Ferrara (1999) estimates are adopted.

The other case is that the galaxy loses part of its ISM, following each event of star formation. Thus, the outflow rate would be expected to be proportional to the SFR. In Fig. 15, we illustrate how the infall models of Fig. 8 are altered by outflows of this type: if the ratio of outflow and SFRs is 1, 2 or 5, the metallicities are reduced by 0.15, 0.3 and 0.75 dex, respectively. The effective yields are reduced by 0.3, 0.5 and 1.1 dex. Since in these models we use a constant star formation time-scale, the gas fractions do not vary with galaxy mass. Thus, both the mass–metallicity and mass–yield relations are essentially modified by a multiplicative factor. Note that the outflows will also lower the gas fractions.

The reduction factor of the effective yield depends strongly on the star formation time-scale and the ratio of outflow rate and SFR, but much less on the infall time-scale, and the exponent x of the SFR, as presented in Fig. 16. Since suitable models have star formation time-scales of about 7 Gyr ($a = 2$), we may take from these schematic

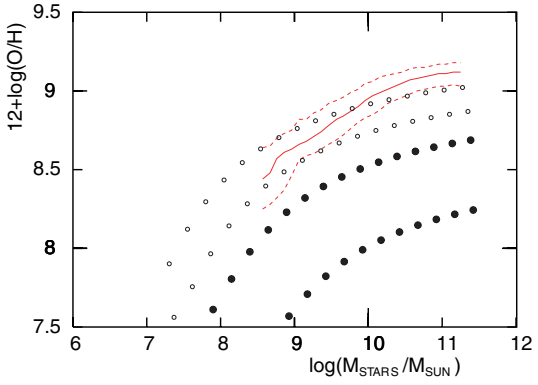

Figure 15. Same as Fig. 8, but with additional gas outflows. The star formation time-scale is 7.5 Gyr ($a = 2$), independent of galaxy mass. The top series of symbols (open ones) are models without outflows; for the ones below the ratio of outflow rate to SFR is taken to be constant at 1, 2 and 5. The symbols indicate the gas fractions, as in Fig. 6.

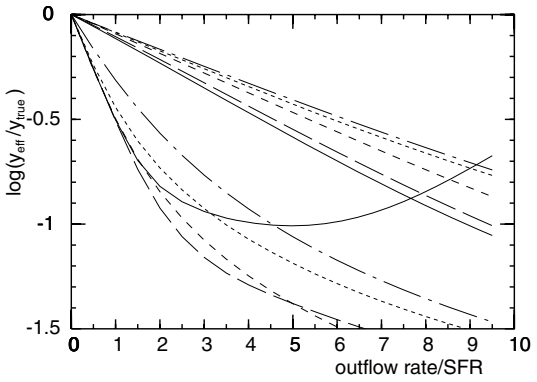

Figure 16. The reduction factors of the effective yield below the true yield for models where the outflow rate is a constant multiple of the SFR. The upper set of curves refers to models with low SFR ($a = 0.5$) and the lower one to those with $a = 4$. The full curves are without infall, the dashed curves are with infall time-scales of 1, 5 and 10 Gyr (shortest dashes). The dash–dotted curves are for an infall time-scale of 5 Gyr, but with a quadratic SFR ($x = 1$).

models that in order to cover the difference of about 1 dex in oxygen abundances and in the yields between massive and dwarf galaxies, the ratio of outflow rate and SFR needs to vary only between 0 and about 5. This number is likely to be near the lower end of this range, because stellar ejecta may also escape directly from dwarf galaxies.

The combination of gas outflows and a variable IGIMF yields a mass–metallicity relation that is steeper than the one produced by either process alone. On the other hand, the presence of strongly fluctuating star formation in dwarf galaxies leads to higher yields – as shown in Section 4.4 – which counteracts the effects of the variable IGIMF and thus gives a flatter mass–metallicity relation. Thus, chemical evolution models with parametrized recipes would not be sufficient to discriminate between the three aspects. To further quantify this is beyond the scope of the present work, which focuses on the consequences of a variable IGIMF on the chemical properties of galaxies.

5.6 Observational data

To compare our models with the observed mass–metallicity relation, we use the recent observational data of Tremonti et al. (2004) which constitute a rather large and also homogeneous set of data. While our study is not the place to discuss in depth all uncertainties and limitations of this data set, several points need to be addressed: the abundances are estimated from the strong lines, thus without measuring the electron temperature in the ionized gas of each object which would require the observation of the faint diagnostic lines. While this can be used with calibration with photoionization models to obtain oxygen abundances, direct comparison with determinations with measured electron temperatures has shown that strong line methods may overestimate the oxygen abundance by as much as 0.5 dex (cf. Kennicutt, Bresolin & Garnett 2003). Furthermore, the data pertain to the central regions of the galaxies which are likely to be of higher metallicity than the averaged value which the models are designed to compute. The computation of the effective yields requires the knowledge of the gas content of each object, which would need the determination of the mass in stars and gas in neutral, ionized and molecular form. The derivation of the gas fraction is further made more complicated in that such a measure should exclude any gas that does not take part in the star-gas cycle of

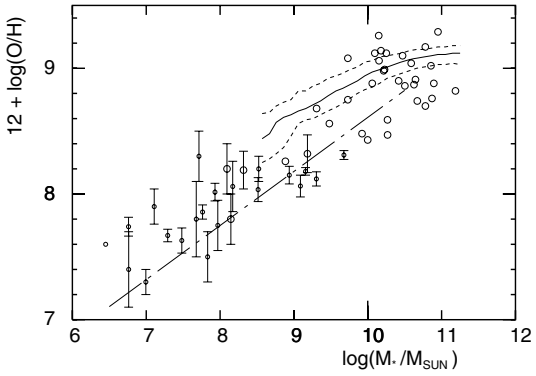

Figure 17. Comparison of the stellar-mass–metallicity relation determined by Tremonti et al. (2004) with abundances for individual gas-rich galaxies from the sample of Köppen & Hensler (2005). Large circles indicate spiral galaxies, and small filled circles are irregulars. The dash–dotted line is a fit to Garnett's (2002) data on oxygen abundances and H I mass.

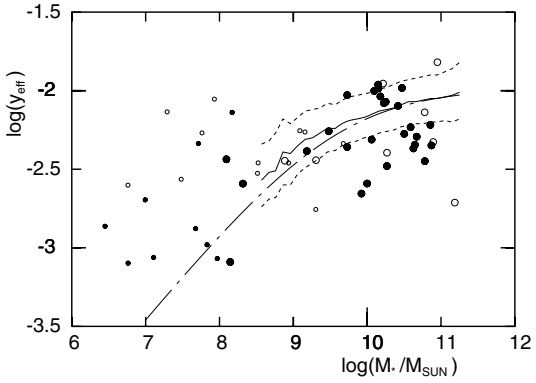

Figure 18. Comparison of the stellar-mass–effective-yield relation derived by Tremonti et al. (2004) with data for individual gas-rich galaxies from the sample of Köppen & Hensler (2005). Large circles indicate the spiral galaxies in the sample of Garnett (2002). A filled symbol indicates that the gas fraction is taken from Garnett (2002). The dot–dashed curve is the mass–yield relation for the galactic wind model from Tremonti et al. (2004).

evolution. Such details of the galaxies are not available for the objects studied by Tremonti et al. (2004); they can determine the gas fraction but by the indirect means of determining the gas surface density from the Hα luminosity via the relation between SFR and gas surface density by Kennicutt (1998). But this verifies that the obtained relation between galaxy mass and effective yields is in good agreement with the data from a number of individual galaxies available in the literature.

We have compared the relations of Tremonti et al. (2004) to data from individual gas-rich galaxies, taken from the literature (for details see Köppen & Hensler 2005) for different objects than used in their comparison. In most of these galaxies, abundances are determined by measuring the electron temperature of the H II gas. As shown in Fig. 17, these individual data show oxygen abundances systematically lower by about 0.3 dex, which is in line with the findings of Kennicutt et al. (2003) in M 101. This is also in agreement with the results by Yin et al. (2006) who compared the oxygen abundances for 531 spectra of star-forming galaxies from the SDSS, based on the direct determination of electron temperatures from the [O III] 5007/4363 line ratio with the Bayesian estimates via strong lines by Tremonti et al. (2004). They find that in about half of the sample the strong-line technique overestimated the abundance by 0.3 dex (their fig. 2), which is correlated to the nitrogen-to-oxygen abundance ratio. In the framework of our models, such an offset could be accounted for by a slightly higher value of $\beta = 2.2$, for instance. Such a change would still be well within the range of acceptable values for this parameter. Merely for comparison, we also plot the relation of H I mass and metallicity by Garnett (2002).

We also compare the effective oxygen yields. Fig. 18 shows that the mass–yield relation from Tremonti et al. (2004) is quite compatible with individual measurements, as was also shown by them by their choice of samples from the literature. A slight tendency to give higher values is also apparent in fig. 8 of Tremonti et al. (2004). There is an appreciable dispersion for a given galactic mass, especially for masses below about $10^8\,M_\odot$. But despite this dispersion, there is a strong tendency for small galaxies to also have low effective yields. Such a feature may be the consequence of a galactic wind scenario as proposed by Tremonti et al. (2004) as well as a signature for a variable IGIMF. One notes that most of the galaxies less massive than $10^9\,M_\odot$ have higher effective yields than predicted by the galactic wind model adopted by Tremonti et al. (2004). The same holds true for our models, of course. Apart from larger uncertainties in the observational data expected from these dwarf galaxies, and the possibility that in these objects the true gas content could have been overestimated due to the presence of H I envelopes [cf. the example of Leo A discussed by Köppen & Hensler (2005)], our model offers a possible physical explanation for such a trend: bursts of intense star formation result in higher yields and higher metallicities than continuous star forming to the same present gas fraction. Nearby dwarf galaxies have quite bursty star formation histories (Grebel 2001), which would tend to favour such an interpretation. Detailed studies of individual galaxies will be necessary to confirm this possibility.

5.7 Scatter in the relations

There is a substantial spread about the mass–metallicity relation, and an even larger one about the mass–gas-fraction relation. It is not the aim of this work to model this scatter, nor to provide physical explanations. But the chemical models permit to make the following statement: one could account for the spread in the gas fractions (Fig. 10) by invoking, for instance, an intrinsic variation of a factor of 2 in the star formation time-scale for galaxies of the same mass, as indicated by the three series of models. The spread of the oxygen abundances from these models in Fig. 11 is somewhat larger than the dispersion found by Tremonti et al. (2004). Because of the relationship $Z = y\ln(f_{\rm gas})$ between metallicity and fraction which exists in a closed-box model but is still closely valid in monotonic infall models, an increase in $\ln(f_{\rm gas})$, caused by a decrease in the SFR, gives rise to an increase in metallicity. In our models with a variable IGIMF, the lower SFR implies a smaller yield, thus the metallicity does not increase as much as if the yield were constant. While this can be seen in the results, it could constitute a possible test for the validity of our scenario: provided that gas fractions and abundances can be measured with sufficient accuracy so as to determine genuine differences in individual objects, and if a correlation between deviations in abundances and gas fractions is found, our scenario would predict that the deviations in abundance should be less than in gas fractions. It is obvious that this quite subtle effect is not an easy test.

If one assumed a relation between galactic H I mass and the gas fraction in our sample of individual galaxies, the deviations from this relation are correlated with the deviations of the oxygen abundances

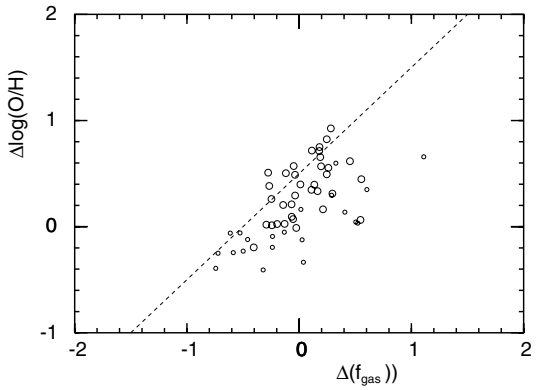

Figure 19. The deviations of the oxygen abundances from the mean mass–metallicity relation of Garnett (2002) as a function of the deviations of the logarithmic gas fractions from the assumed relation shown in Fig. 9. Large circles indicate the spiral galaxies in the sample of Garnett (2002). The dotted line indicates the slope of unity which would be expected for closed-box chemical evolution with the same constant effective yield.

from the mass–metallicity relation of Garnett (2002), as shown in Fig. 19. This correlation is only marginally significant (correlation coefficient 0.6 for all objects and 0.5 for the spiral galaxies); but as the dotted line indicates, the trend is in good agreement to what one should expect if all galaxies had the same yield and evolved as nearly closed boxes.

6 CONCLUSIONS

The closed-box model, as well as the models with monotonically decreasing infall, provides a remarkable match to the observed median mass–metallicity relation. This is in strong contrast to models with a constant IMF which all have the same effective yield for all galactic masses and all star formation time-scales, and therefore do not provide a reasonable match. In the case of the infall models the effective yields also match the observed relation very reasonably. The match with the observations is independent of the adopted infall time-scale. For models with a starburst, the resulting IGIMF includes a higher number of massive stars. In comparison to continuous star formation, the average metal yield will therefore be larger. This leads to both higher oxygen abundances and higher effective yields in strong starbursts. It must be noted that the rather schematic model of starbursts used here mainly shows the tendency of the results for extreme burst-type star formation histories. Regardless of the details, it is important that these results predict higher metallicities and higher oxygen yields for galaxies with strongly fluctuating star formation histories. Our models – closed box and infall – thus constitute an upper limit of the effects due to a variation of the IGIMF on the SFR. By combining the effects of gas outflows and a variable IGIMF, a steeper mass–metallicity relation would be achieved than the ones produced by either process alone. But in dwarf galaxies, strong fluctuations in star formation would lead to higher yields thereby compensating this and flattening the stellar-mass–metallicity relation to the observed slope.

It may be possible to test our model in more detail provided that gas fractions and abundances can be measured with sufficient accuracy so as to determine genuine differences in individual objects. If a correlation between deviations in abundances and gas fractions is found, our scenario would predict that the deviations in abundances should be less than in gas fractions.

The idea of a SFR-dependent IGIMF provides a most attractive way to explain the observed relations between metallicity and galactic mass as well as the one between effective yield and galactic mass. The main effect at work is the lowering of the effective upper mass limit of stars for low star formation rates, which reduces the number of supernovae of type II.

Our results demonstrate a good agreement with the mass–metallicity data, even for $\beta = 2$, without needing to invoke outflows. This may suggest that the importance of outflows for shaping the mass–metallicity relation may need reconsideration. Thus, the oxygen yield becomes a sensitive function not only of the SFR but also of the cluster MF power-law index β. Low-mass galaxies therefore appear chemically less-evolved than massive galaxies despite having the same ages.

If one wanted to explain the mass–metallicity relation by an explicit variation of the slope of the IGIMF on galaxy mass, one would need to vary the exponent α above about 1.5 $M_\odot$ from 2.5 for galaxy masses of about 5×10^8 $M_\odot$ to 2.3 for 2×10^{11} $M_\odot$, which is the range of the data covered by the observations of Tremonti et al. (2004). These changes of the IGIMF slope α correspond to the 'minimal' scenario proposed in Weidner & Kroupa (2005).

In a recent paper, Lee et al. (2006) investigate the mass–metallicity relation with a more recent sample of dwarf galaxies with *Spitzer* data. The sample is, in principle, in agreement with the data we use and form an extension to lower galactic masses. They find a rather flat mass–yield relation noting it 'is difficult to explain, if galactic winds are ubiquitous in dwarf galaxies'. Therewith, they indicate that other solutions rather than galactic winds might still be possible. Here, the flat stellar-mass–yield relation is explainable with a SFR-dependent IGIMF by invoking bursty star formation histories for dwarfs.

Furthermore in another recent paper (Dalcanton 2006), it has been shown that neither outflows nor accretion of low-metallicity gas can reproduce the low effective yields observed in low-mass galaxies. It is conceivable that a variable IGIMF could help to explain this problem.

Our models indicate that massive spirals and ellipticals should show less variations in the IGIMF and thus metallicities due to their high average SFR. This is observed in nearby galaxies as is seen in fig. 9 in Garnett (2004) or in the sample of 53 000 galaxies plotted in fig. 6 in Tremonti et al. (2004). The direct consequence of a dependence of the IGIMF on the SFR is a strong dependence of the oxygen abundance on the mass of a galaxy. It alone would already suffice to explain the observed mass–metallicity relation. Thus, it would impose lesser demands on the loss of metals by outflows.

To verify whether the SFR dependence of the IGIMF could indeed be the origin or at least part of the explanation of the mass–metallicity relation of galaxies, we are in the process of comparing model predictions with other observational properties, among them the abundances of other elements. The variation of the IGIMF strongly affects the massive stars but only weakly the intermediate mass stars. Thus, we would expect that elements produced only in massive stars will vary as strongly as oxygen, but that elements with a strong contribution from intermediate mass stars – such as carbon, nitrogen and iron – will vary to a lesser extent. This will be the subject of a future study.

ACKNOWLEDGMENTS

We thank Simone Recchi, for discussions, and our anonymous referee for numerous detailed comments. This research has been

supported by DFG grant KR1635/3 and the Chilean FONDECYT grant 3060096.

REFERENCES

Bell E. F., McIntosh D. H., Katz N., Weinberg M. D., 2003, ApJS, 149, 289
Brinchmann J., Charlot S., White S. D. M., Tremonti C., Kauffmann G., Heckman T., Brinkmann J., 2004, MNRAS, 351, 1151
Brodie J. P., Huchra J. P., 1991, ApJ, 379, 157
Chiosi C., 1980, A&A, 93, 206
Conselice C. J., 2006, ApJ, 638, 686
Dalcanton J. J., 2006, ApJ, in press (astro-ph/0608590)
De Lucia G., Kauffmann G., White S. D. M., 2004, MNRAS, 349, 1101
Dekel A., Silk J., 1986, ApJ, 303, 39
Egusa F., Sofue Y., Nakanishi H., 2004, PASJ, 56, L45
Elmegreen B. G., 2000, ApJ, 530, 277
Elmegreen B. G., 2006, ApJ, 648, 572
Faber S. M., 1973, ApJ, 179, 731
Figer D. F., 2005, Nat, 434, 192
Freyer T., Hensler G., Yorke H. W., 2003, ApJ, 594, 888
Garnett D. R., 2002, ApJ, 581, 1019
Garnett D. R., 2004, in Esteban C., García-Lopez R., Herrera A., Sanchez F., eds, Cosmochemistry. The Melting Pot of the Elements Element Abundances in Nearby Galaxies. p. 171
Glazebrook K. et al., 2003, ApJ, 587, 55
Goodwin S. P., Pagel B. E. J., 2005, MNRAS, 359, 707
Grebel E. K., 2001, Astrophys. Space Sci. Suppl., 277, 231
Hartmann L., Ballesteros-Paredes J., Bergin E. A., 2001, ApJ, 562, 852
Heavens A., Panter B., Jimenez R., Dunlop J., 2004, Nat, 428, 625
Henry R. B. C., Edmunds M. G., Köppen J., 2000, ApJ, 541, 660
Hunter D. A., Elmegreen B. G., Dupuy T. J., Mortonson M., 2003, AJ, 126, 1836
Köppen J., Arimoto N., 1991, A&AS, 87, 109
Köppen J., Edmunds M. G., 1999, MNRAS, 306, 317
Köppen J., Hensler G., 2005, A&A, 434, 531
Kennicutt R. C. Jr, 1983, ApJ, 272, 54
Kennicutt R. C. Jr, 1998, ARA&A, 36, 189
Kennicutt R. C. Jr, Bresolin F., Garnett D. R., 2003, ApJ, 591, 801
Koen C., 2006, MNRAS, 365, 590
Kroupa P., 2001, MNRAS, 322, 231
Kroupa P., 2002, Sci, 295, 82
Kroupa P., Weidner C., 2003, ApJ, 598, 1076
Kroupa P., Tout C. A., Gilmore G., 1993, MNRAS, 262, 545
Lada C. J., Lada E. A., 2003, ARA&A, 41, 57
Lee H.-C., Gibson B. K., Flynn C., Kowata D., Beasley M. A., 2004, MNRAS, 353, 113
Lee H., Skillman E. D., Cannon J. M., Jackson D. C., Gehrz R. D., Polomski E. F., Woodward C. E., 2006, ApJ, 647, 970
Lequeux J., Peimbert M., Rayo J. F., Serrano A., Torres-Peimbert S., 1979, A&A, 80, 155
Mac Low M.-M., Ferrara A., 1999, ApJ, 513, 142
Maeder A., 1992, A&A, 264, 105
Massey P., 2002, ApJS, 141, 81
Massey P., 2003, ARA&A, 41, 15
Massey P., Hunter D. A., 1998, ApJ, 493, 180
Matteucci F., 1986, PASP, 98, 973
Matteucci F., Francois P., 1992, A&A, 262, L1
Meynet G., Maeder A., 2002, A&A, 390, 561
Miller G. E., Scalo J. M., 1979, ApJS, 41, 513
Naab T., Ostriker J. P., 2006, MNRAS, 366, 899
Oey M. S., Clarke C. J., 2005, ApJ, 620, L43
Parker J. W., Zaritsky D., Stecher T. P., Harris J., Massey P., 2001, AJ, 121, 891
Piskunov A. E., Belikov A. N., Kharchenko N. V., Sagar R., Subramaniam A., 2004, MNRAS, 349, 1449
Recchi S., Hensler G., Angeretti L., Matteucci F., 2006, A&A, 445, 875
Reid I. N., Gizis J. E., Hawley S. L., 2002, AJ, 124, 2721
Salpeter E. E., 1955, ApJ, 121, 161
Scalo J. M., 1986, Fundam. Cosm. Phys., 11, 1
Silich S. A., Tenorio-Tagle G., 1998, MNRAS, 299, 249
Silich S. A., Tenorio-Tagle G., 2001, ApJ, 552, 91
Sirianni M., Nota A., Leitherer C., De Marchi G., Clampin M., 2000, ApJ, 533, 203
Sirianni M., Nota A., De Marchi G., Leitherer C., Clampin M., 2002, ApJ, 579, 275
Skillman E. D., Kennicutt R. C. Jr, Hodge P. W., 1989, ApJ, 347, 875
Talbot R. J., Arnett W. D., 1971, ApJ, 170, 409
Thielemann F.-K., Nomoto K., Hashimoto M.-A., 1996, ApJ, 460, 408
Thomas D., Greggio L., Bender R., 1998, MNRAS, 296, 119
Tremonti C. A. et al., 2004, ApJ, 613, 898
Unavane M., Wyse R. F. G., Gilmore G., 1996, MNRAS, 278, 727
van den Hoek L. B., Groenewegen M. A. T., 1997, A&AS, 123, 305
Venn K. A., Irwin M., Shetrone M. D., Tout C. A., Hill V., Tolstoy E., 2004, AJ, 128, 1177
Weidner C., Kroupa P., 2004, MNRAS, 348, 187
Weidner C., Kroupa P., 2005, ApJ, 625, 754
Weidner C., Kroupa P., 2006, MNRAS, 365, 1333
Weidner C., Kroupa P., Larsen S. S., 2004, MNRAS, 350, 1503
Woosley S. E., Weaver T. A., 1995, ApJS, 101, 181
Wyse R. F. G., Gilmore G., Houdashelt M. L., Feltzing S., Hebb L., Gallagher J. S., Smecker-Hane T. A., 2002, New Astron., 7, 395
Yin S. Y., Liang Y. C., Hammer F., Brinchmann J., Zhang B., Deng L. C., Flores H., 2006, A&A, in press (astro-ph/0610068)
Zaritsky D., Kennicutt R. C. Jr, Huchra J. P., 1994, ApJ, 420, 87
Zhang Q., Fall S. M., 1999, ApJ, 527, L81

This paper has been typeset from a TEX/LATEX file prepared by the author.